

Electronic Supplementary Information for:

Evidence of Double Layer/Capacitive Charging in Carbon Nanomaterial-Based Solid Contact Polymeric Ion-Selective Electrodes

Maria Cuartero^a, Josiah Bishop^b, Raymart Walker^b, Robert G. Acres^c, Eric Bakker^a, Roland De Marco^{b,d,e} and Gaston A. Crespo^{a,}*

^aDepartment of Inorganic and Analytical Chemistry, University of Geneva, Quai Ernest-Ansermet 30, CH-1211 Geneva, Switzerland.

^bFaculty of Science, Health, Education and Engineering, University of the Sunshine Coast, 90 Sippy Downs Drive, Sippy Downs, Queensland 4556, Australia.

^cAustralian Synchrotron, 800 Blackburn Road, Clayton, VIC 3168, Australia.

^dSchool of Chemistry and Molecular Biosciences, The University of Queensland, Brisbane, Queensland 4072, Australia.

^eDepartment of Chemistry, Curtin University, GPO Box U1987, Perth, Western Australia 6109, Australia.

*Corresponding Author: gaston.crespo@unige.ch

Table of content

	Page
1. Experimental	SI-3
Materials, reagents and instruments	SI-3
Electrode preparation	SI-3
Electrochemical polarization	SI-3
Synchrotron radiation-X-ray photoelectron spectroscopy (SR-XPS) measurements	SI-4
2. Theory of Photoionization and Standardization of SR-XPS Line Intensities	SI-6
3. Peak Assignment in SR-XPS spectra	SI-7
4. Supporting figures	SI-8
Fig. S1- Difference between POT and f-MWCNTs layers	SI-8
Fig. S2- Control experiments for MWCNTs and POT layers	SI-9
Fig. S3- SR-XPS C 1s spectra for MWCNTs..	SI-10
Fig. S4- SR-XPS O 1s spectra for MWCNTs.	SI-11
Fig. S5- SR-XPS N 1s spectra for ODA MWCNTs.	SI-12
Fig. S6- Ellipsometry.	SI-13
Fig. S7- Nyquist plot (EIS).	SI-14
Fig. S8- Cyclic voltammetry of f-MWCNTs film.	SI-15
Fig. S9- SXR-AS control depth profiling.	SI-16
Fig. S10- SR-XPS F 1s, Na +s and C 1s spectra for PVC / ODA MWCNTs / GC.	SI-17
Fig. S11- VB spectra for PVC / ODA MWCNTs / GC.	SI-18
5. References	SI-19

1. Experimental Details

Materials, reagents and instruments

Multi-walled carbon nanotubes (MWCNTs, >95% wt. purity, 0.5-200 μm length and 30-50 nm diameter, M4905) were purchased from HeJi, Inc (Zengcheng City, China). Tetrahydrofuran (THF), thionyl chloride (SOCl_2), octadecylamine (ODA), bis(2-ethylhexyl) sebacate (DOS), sodium tetrakis[3,5-bis-(trifluoromethyl)phenyl]borate (NaTFPB), sulphuric acid (97%), nitric acid (65%), poly(vinyl-chloride) (PVC, high molecular weight), and sodium chloride (analytical grade) were purchased from Sigma-Aldrich. Glassy carbon (GC) coupons (Sigradur G, $10 \times 10 \times 1$ mm) were purchased from HTW (Germany). The ODA functionalized MWCNTs, which are soluble in THF and easily cast onto electrodes, were synthesized according to the method of Yuan et al. [1]

Ellipsometric experiments were made using an ellipsometer (Multiskop, Optrel) with a 632.8 nm Laser. A volume of 20 μL of the corresponding membrane cocktail was deposited by drop casting (1500 rpm) on the glassy carbon plates. The ellipsometric parameters (Δ and Ψ) were recorded as a function of the angle of incidence from 60° to 75° at every 0.5° for bare plate as well as different deposited membranes. The software Matlab_R2012b was used for the simulations to obtain first the refractive index of the GC plates and then the thicknesses of the different membranes.

For impedance experiments a PGSTAT 302N (Metrohm Autolab B.V., Utrecht, The Netherlands) combined with a FRA32M module controlled by Nova 1.11 software (supplied by Autolab) was used. (Parameters used: from 100 KHz to 0.1 Hz, sinusoidal excitation signal (single sine), $\Delta E_{ac}=10$ mV, $E_{dc}=0.02$ V (OCP vs. Ag/AgCl wire). Cd calculated at 0.1 Hz ($Z''=3198 \Omega$) is $\sim 500 \mu\text{F}$).

Electrode preparation

1 mg of ODA functionalized MWCNTs was dissolved in 1 mL of THF. A volume of 100 μL is deposited by drop casting ($10 \mu\text{L} \times 10$ times) onto the GC coupons, resulting in a film of ~ 300 nm of thickness (measured by ellipsometry).

The PVC membrane was prepared by dissolving 32 mg of PVC, 64 mg of DOS and 3.55 mg of NaTFPB (40 mmol kg^{-1}) in 1 mL of THF. Subsequently, a dilution of this cocktail ($50 \mu\text{L} + 150 \mu\text{L}$ of THF) was prepared. Thin layer membranes (~ 160 nm thickness measured by ellipsometry) were spin coated (1500 rpm) onto the ODA functionalized MWCNT GC electrode using a volume of 20 μL of the diluted cocktail and a KW-4A (Chemat Technology Inc., UK) spin coater rotated at 1500 rpm for 1 min.

Electrochemical polarization

The PVC membrane/ODA functionalized MWCNT GC coupon was accommodated within a demountable Teflon electrochemical cell fitted with a platinum counter electrode (6.0331.010 model,

Metrohm, Switzerland) and a double-junction Ag/AgCl/3 M KCl/1 M LiOAc reference electrode (6.0726.100 model, Metrohm, Switzerland). Electrochemical charging of the ODA MWCNT film was performed using a PGSTAT 128N potentiostat (Metrohm Autolab B.V., Utrecht, The Netherlands) controlled by Nova 1.11 software running on a computer. The electrochemical cell was polarized at 0.6 V for 180 s in 10 mM NaCl solution. Thereafter, the cell was disassembled, and the treated coupons were soaked for 30 minutes in deionized water to remove adsorbed/absorbed electrolyte and other impurities.

Synchrotron radiation-X-ray photoelectron spectroscopy (SR-XPS) measurements

With regard to the argon ion depth profiling of electrochemically charged f-MWNT/PVC systems at the Elettra materials science beamline (MSB) and the Australian Synchrotron (AS) soft X-ray (SXR) beamline. It is important to note that the bending magnet Elettra MSB yielded diminished counting statistics for the SR-XPS F 1s core level spectra in transported sodium tetrakis[3,5-bis-(trifluoromethyl)phenyl] borate (NaTFPB) and could only be used to access the much weaker Na 2p core level spectra at about 30 eV due to the photon energy beam limit of 1,000 eV, while the AS SXR undulator beamline yielded considerably improved counting statistics for SR-XPS F 1s core level spectra and accessed the much stronger Na 1s core level spectra in NaTFPB. By contrast, the Elettra MSB could measure more reliably valence band (VB) spectra owing to an ability to access a lower photon energy of 30 eV, while the AS SXR beamline could only reach a lower beam energy of 100 eV. Accordingly, argon ion depth profiles of SR-XPS F 1s, Na 1s and other core level spectra were reported from the AS SXR beamline results, while argon ion depth profiles of the VB spectra were measured at the Elettra MSB facility.

SR-XPS survey and high resolution spectra were recorded on the soft X-ray beamline (SXR) at the AS light source in Melbourne, Australia. High resolution core level spectra were recorded at a photon energy that was approximately 50 eV above the core level absorption edge, so as to enhance photoemission and the concomitant sensitivity of SR-XPS measurements, and all measurements were performed at an angle of 55° with respect to the sample normal. This beamline utilizes an insertion device based on an elliptically polarized undulator providing a flux between 5×10^{11} and 3×10^{12} photons/200 mA at the sample at 400 eV. The optimal energy range of the beamline is between 90 to 2000 eV with a resolution ($E/\Delta E$) of 5,000 to 10,000 with a beam size of 0.6 mm \times 0.6 mm. The end-station was constructed by OmniVac and PreVac using a SPECS Phoebos 150 hemispherical electron energy analyzer in conjunction with photodiode and drain current detectors. The analyzer chamber was maintained at 1×10^{-9} mbar or better and the storage ring was operated in the decay mode. The binding energy scale at each photon energy was calibrated against Au 4f_{7/2} peak at 83.95 eV from a gold foil standard.

Valence band (VB) spectra were recorded using a photon energy of 40 eV at the Materials Science beamline (MSB) at the Elettra synchrotron light source in Trieste Italy. The MSB end-station comprises an ultrahigh vacuum instrument (10^{-10} mbar base pressure, and was maintained at 5×10^{-9} mbar or better during measurements) that is equipped with a Specs Phoibos 150 multichannel electron energy analyzer along with an argon gas inlet and argon ion sputtering gun. The binding energy scale of the SR-XPS spectra was calibrated against the Au Fermi edge using a gold foil standard.

CasaXPS was used to fit Gaussian/Lorentzian peaks together with a Shirley background correction, so as to deconvolute spectra comprising multiple components. SR-XPS intensity data was corrected for photon energy effects on the photoabsorption cross-sections and angular asymmetry parameters of core level orbitals together with electron kinetic energy effects on inelastic scattering of photoelectrons and spectrometer transmission to provide percentages of total intensity/mol.% data for detected elements (see the Theory of Photoionization and Standardization of SR-XPS Line Intensities section below).

Since the PVC membrane/ODA functionalized MWCNTs had a tendency to outgas in the UHV chamber of the SXR and MSB end-stations, all samples, both treated and untreated, were placed in a vacuum desiccator for several hours (at least 8 hours) prior to introduction to the UHV system.

Argon ion sputtering of samples was performed at 500 V, 25 mA and 2×10^{-6} mbar of argon (MSB at Elettra) as well as 600 V, 5 mA and 5×10^{-6} mbar (SXR at the AS). From the sputtering of 2×200 nm thick PVC layers at MSB at Elettra and separate 200 nm thick PVC and ODA MWCNT films on GC substrates at the SXR at the AS, it was found that 16-18 mins. of sputtering was required to remove PVC and reach the underlying GC substrate (MSB at Elettra) while 50-60 mins. of sputtering was needed to remove the separate PVC and ODA MWCNT films and reach the GC substrate at the SXR at the AS. Hence, the average sputter rate of the argon ion guns were estimated to be 12 ± 1 nm min^{-1} (MSB at Elettra) and 3.7 ± 0.4 nm min^{-1} (SXR at the AS), noting that these estimates are relevant to both PVC and ODA MWCNT. These figures were used to set the depth scale of the X-axis of depth profiles.

2. Theory of Photoionization and Standardization of SR-XPS Line Intensities

The photoelectron line intensity in X-ray photoelectron spectroscopy (XPS) is given by:

$$I = I_0 \times \sigma_i \times T_i \times \lambda_i \times N_i \quad (1) [2]$$

where I is the experimentally determined photoelectron line intensity, I_0 is the incident photon flux on the sample that is considered to be constant, σ_i is the differential cross-section, T_i is the transmission function of the electron spectrometer, λ_i is the inelastic mean-free path of the photoelectrons and N_i is the volume density of the detected element.

The factors σ_i , T_i , and λ_i are represented by the following expressions:

$$\sigma_i = \sigma(h\nu) \times \left\{ \left(1 + \frac{\beta(h\nu)}{2} \left[\frac{3}{2} \times \sin^2 \theta - 1 \right] \right) \right\} \quad (2) [2]$$

$$T_i = \frac{1}{\sqrt{E_k}} \quad (3) [3]$$

$$\lambda_i = 49 \left(\frac{1}{(E_k)^2} \right) + 0.11 \sqrt{E_k} \quad (4) [4]$$

where $\sigma(h\nu)$ is the photon energy dependent Scofield total photoabsorption cross-section of the core level atomic orbital, $\beta(h\nu)$ is the photon energy dependent angular asymmetry parameter of the core level atomic orbital, and E_k is kinetic energy of the photoelectrons in eV from the core level atomic orbital. Note that the photon energy dependent values of $\sigma(h\nu)$ and $\beta(h\nu)$ can be sourced from the URL, <https://vuo.elettra.eu/services/elements/WebElements.html>, while T_i is approximated effectively by this function since all core level SR-XPS spectra were recorded at a photon energy that is approximately 50 eV above the core level edge, or at an approximately constant electron kinetic energy of about 50 eV.

Substitution of Equations (2), (3) and (4) into Equation (1) yields the following expression:

$$I = I_0 \times \sigma(h\nu) \times \left\{ \left(1 + \frac{\beta(h\nu)}{2} \left[\frac{3}{2} \times \sin^2 \theta - 1 \right] \right) \right\} \times \frac{1}{\sqrt{E_k}} \times \left\{ 49 \left(\frac{1}{(E_k)^2} \right) + 0.11 \sqrt{E_k} \right\} N_i \quad (5)$$

From Equation (5), it can be shown that a division of each photoelectron line intensity by the factor, $\sigma(h\nu) \times \left\{ \left(1 + \frac{\beta(h\nu)}{2} \left[\frac{3}{2} \times \sin^2 \theta - 1 \right] \right) \right\} \times \frac{1}{\sqrt{E_k}} \times \left\{ 49 \left(\frac{1}{(E_k)^2} \right) + 0.11 \sqrt{E_k} \right\}$, and normalization of all factorized photoelectron line intensities, I' , yields the mol.% of x elements detected by XPS, viz.

$$I' = \frac{I}{\sigma(h\nu) \times \left\{ \left(1 + \frac{\beta(h\nu)}{2} \left[\frac{3}{2} \times \sin^2 \theta - 1 \right] \right) \right\} \times \frac{1}{\sqrt{E_k}} \times \left\{ 49 \left(\frac{1}{(E_k)^2} \right) + 0.11 \sqrt{E_k} \right\}} \quad (6)$$

$$\text{and } x(\text{mol.}\%) = \frac{I'_x}{\sum_{i=1}^n I'_i} \times 100 = \frac{I_0 N_x}{I_0 \sum_{i=1}^n N_i} \times 100 = \frac{N_x}{\sum_{i=1}^n N_i} \times 100 \quad (7)$$

3. Peak Assignment in SR-XPS spectra

The C 1s core level for raw MWCNTs (see Fig. S3a) shows the graphitic C species at 284.6 eV together with a small peak at about 286.5 eV that is ascribable to a low concentration of C in -C-OH and/or -C=O functionalities. However, the corresponding O 1s spectrum (see Fig. S4a) revealed a single peak at 532.5 eV that is due to O in -C=O functional groups in ketones and/or aldehydes, so the small C 1s shoulder is most probably ascribable to C in -C=O groups. It is clear that oxidation of the MWCNTs (see Fig. S3b for the C 1s core level spectrum) produced three small and high binding energy C 1s shoulders at about 285.5, 287 and 289 eV that are attributable to C in -C-OH, -C=O (ketones and aldehydes) and -COOH functionalities, respectively, noting that the associated O 1s core level spectrum (see Fig. S4b) revealed 2 peaks at 532.5 and 534 eV that are ascribable to O in -C-OH and -C=O functionalities, respectively²⁰. Notably, there has been an increase in the O 1s intensity from several hundred counts on the raw MWCNTs to a few thousand counts on the oxidized MWCNTs (cf., Fig. S4a and S4b), with the aforesaid evidence consistent with the introduction of significant -COOH functionalities that may be functionalized by ODA.

Finally, upon functionalization of oxidized MWCNTs by ODA, it is evident that there has been a significant increase in the relative intensity of the C 1s peak at 285.5 eV (cf., Fig. S3b and Fig. S3c), which corresponds to a convolution of C in -C-N and -C-OH from the oxidized MWCNTs. For the N 1s SR-XPS core level spectrum for ODA functionalized MWCNTs (see Fig. S5), it is evident that there is a -N-C=O (amide) peak at 400.5 eV and a -C=N (imine) peak at 398 eV from the equilibrium tautomer of the ODA amide species. Furthermore, the ratio of amide (400.5 eV peak) to imine (398 eV peak) peak intensities of about 3:1 is consistent with the previously published N 1s core level spectra for the amide-imine tautomers.

4. Supporting Figures

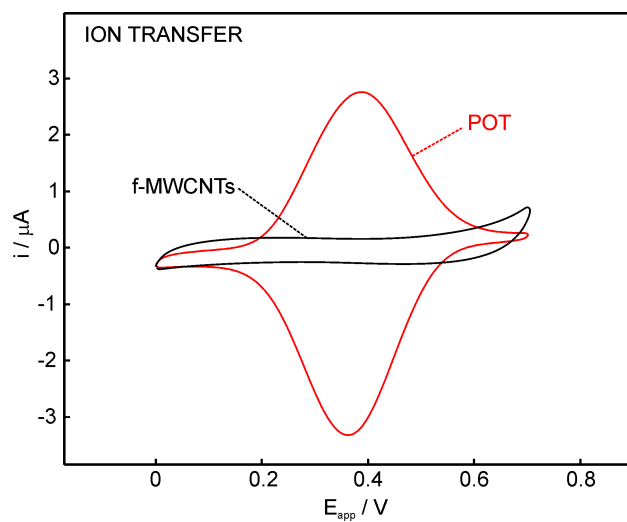


Figure S1. Red cyclic voltammogram: Sodium ion transfer for a system composed of a GC/POT(160 nm of thickness)/polymeric membrane (60 nm of thickness, Na^+R^- : 40 mmol kg^{-1} , DOS and PVC). Black voltammogram: the previous POT layer is replaced by f-MWCNT layer (~ 300 nm). Scan rate: 100 mV s^{-1} and 10 mM NaCl as a background electrolyte.

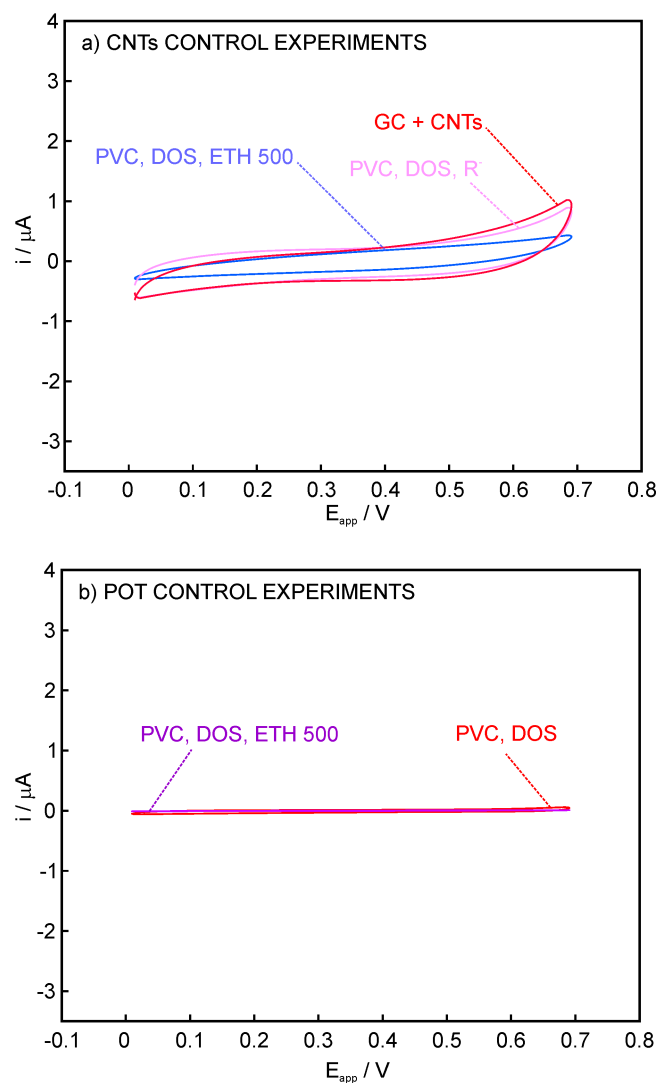


Figure S2. a) Control voltammograms for f-MWCNTs system. Red: GC/f-MWCNTs; Pink: GC/f-MWCNTs/polymeric membrane (160 nm of thickness, Na^+R^- : 40 mmol kg^{-1} , DOS and PVC). Blue: GC/f-MWCNTs/polymeric membrane (160 nm of thickness, R^+R^- : 40 mmol kg^{-1} , DOS and PVC). b) Control voltammograms for POT system. Violet: GC/POT(60 nm of thickness)/polymeric membrane (160 nm of thickness, R^+R^- : 40 mmol kg^{-1} , DOS and PVC). Red: GC/POT(60 nm of thickness)/polymeric membrane (160 nm of thickness, DOS and PVC)

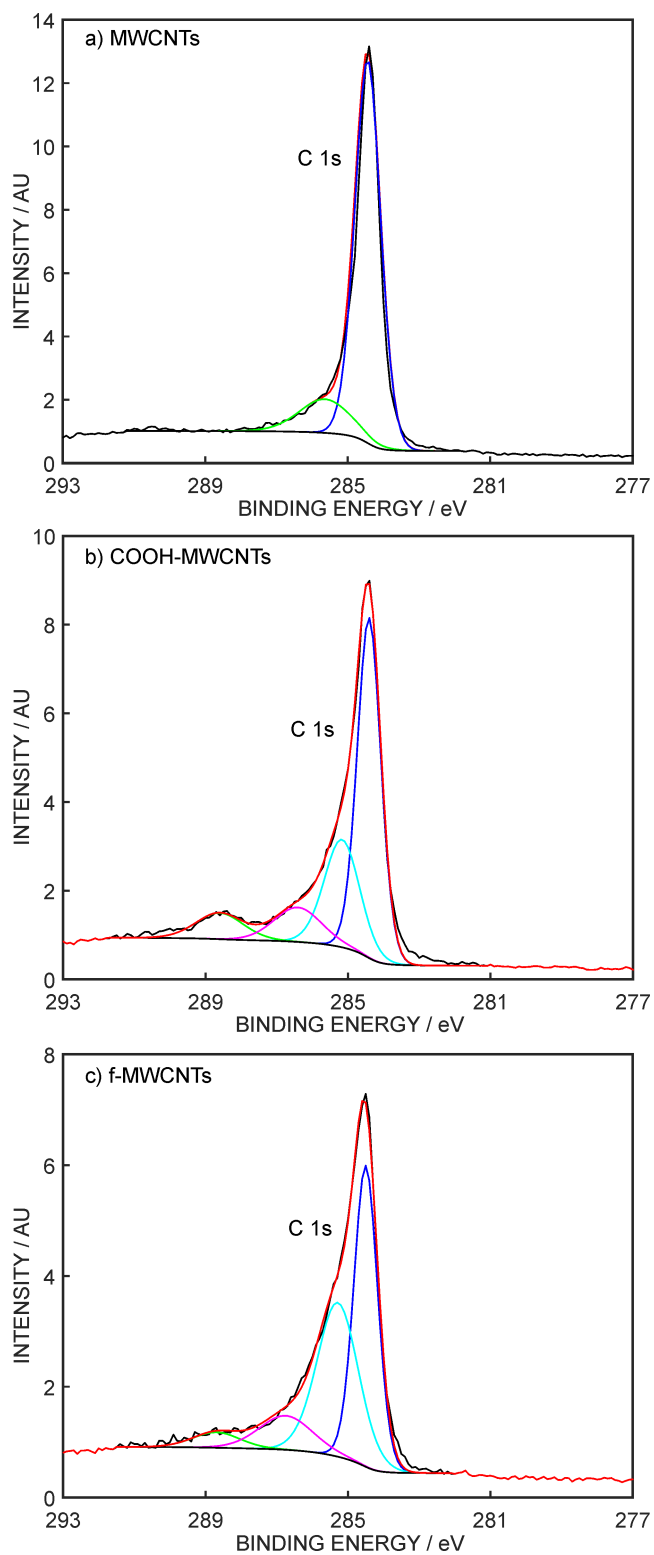


Figure S3. High resolution SR-XPS C 1s spectra for MWCNTs (AU = counts/ 10^3): a) raw and unreacted MWCNTs; b) MWCNTs that have been oxidized to introduce $-\text{COOH}$ functional groups; c) oxidized MWCNTs that have been functionalized with ODA.

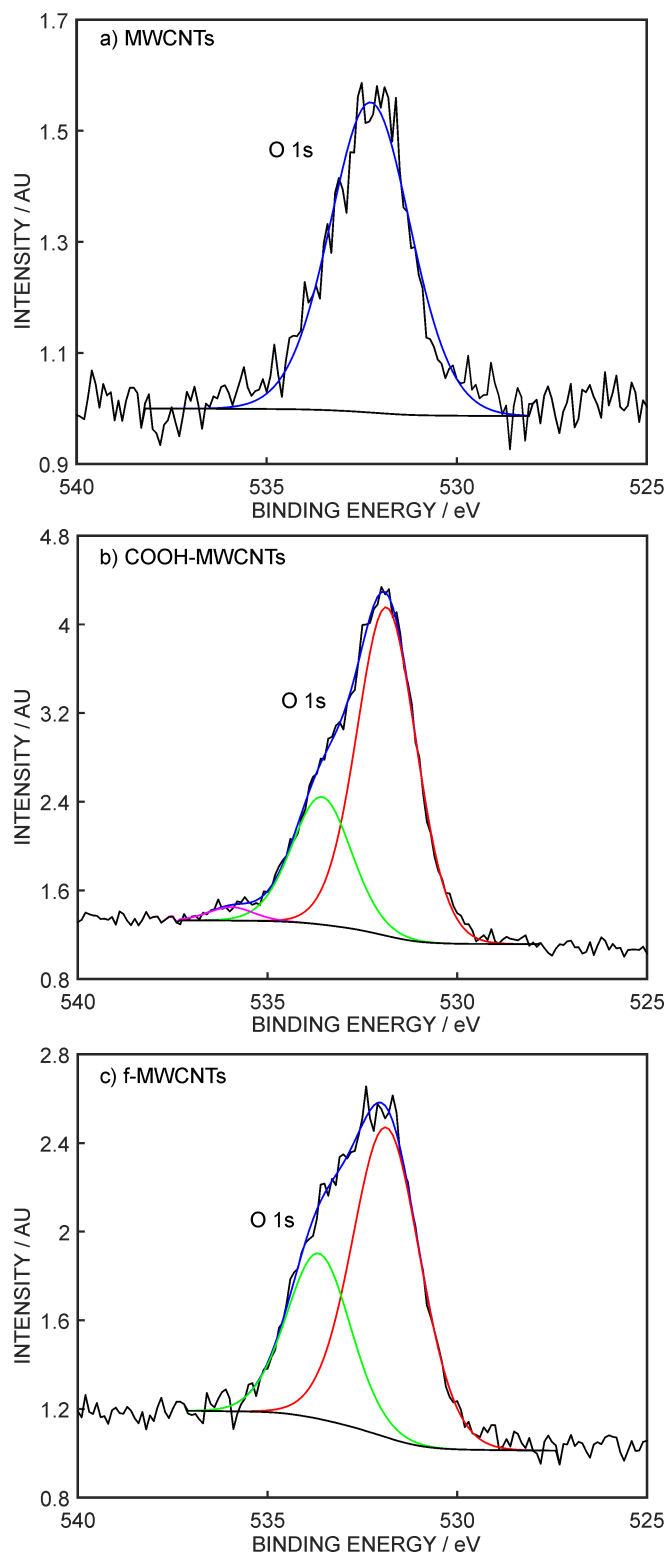


Figure S4. High resolution SR-XPS O 1s spectra for MWCNTs (AU = counts/ 10^3): a) raw and unreacted MWCNTs; b) MWCNTs that have been oxidized to introduce $-\text{COOH}$ functional groups; c) oxidized MWCNTs that have been functionalized with ODA.

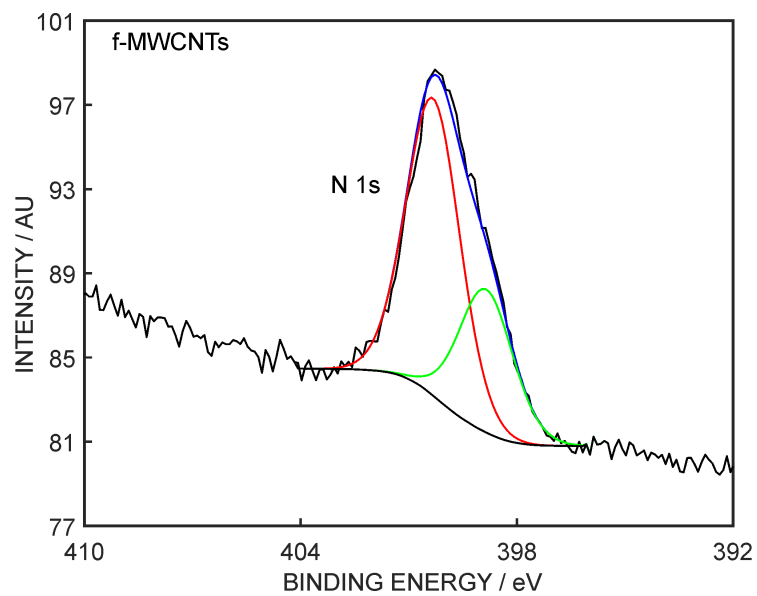


Figure S5. High resolution SR-XPS N 1s spectrum for the ODA functionalization of oxidized MWCNTs (AU = counts/ 10^3).

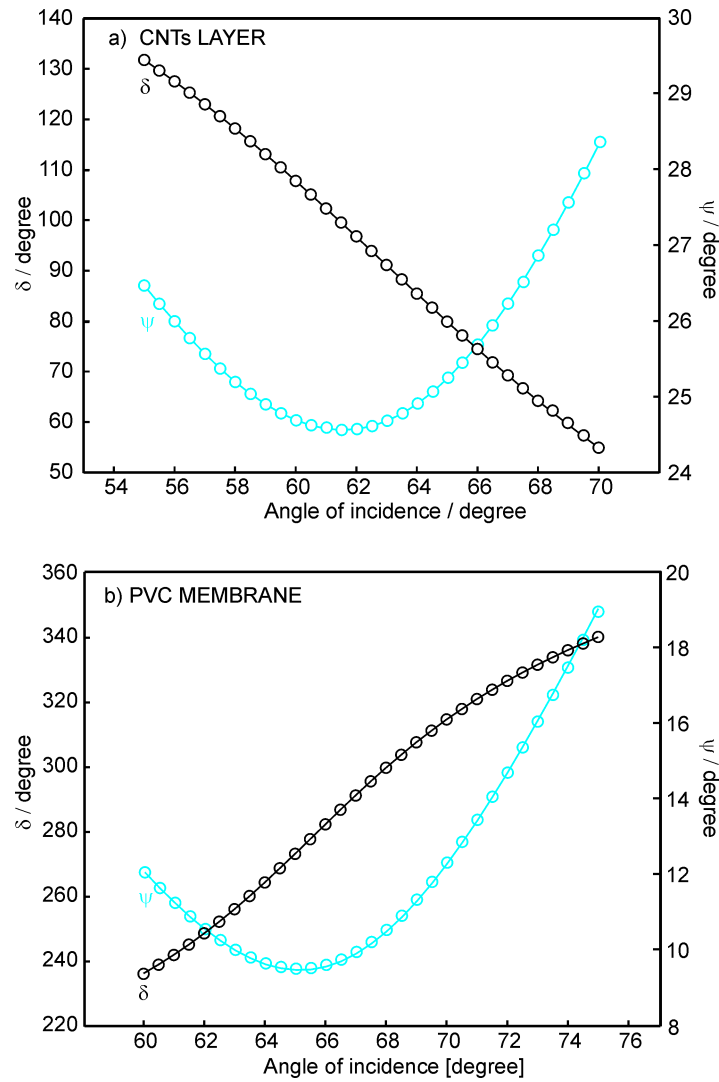


Figure S6. Ellipsometric characterization of (a) a film composed of functionalized CNTs (average thickness of 310 ± 20 nm) and (b) thin membrane composed of Na+R-, PVC and DOS (160 ± 10 nm). Ellipsometric parameters Δ and Ψ are plotted vs. different angle of incidences. Lines correspond to the simulation of the angular dependence of the parameters. N=3

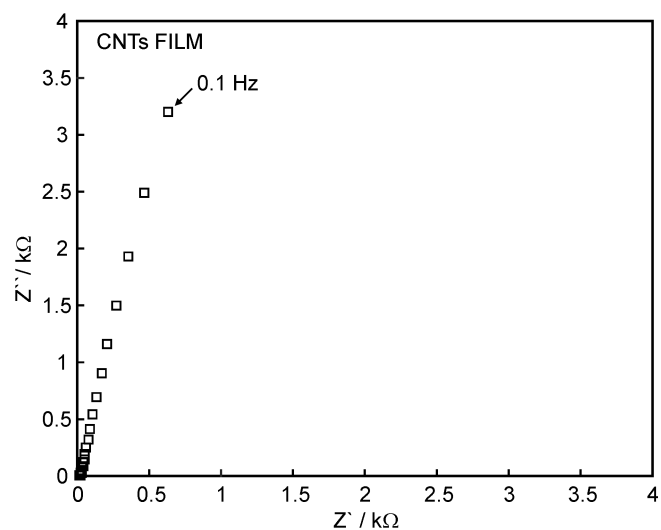


Figure S7. Nyquist plot of f-MWCNTs layer (~ 300 nm). (Parameters used: from 100 KHz to 0.1 Hz, sinusoidal excitation signal (single sine), $\Delta E_{ac}=10$ mV, $E_{dc}=0.02$ V (OCP vs. Ag/AgCl wire). Cd calculated at 0.1 Hz ($Z''=3198 \Omega$) is $\sim 500 \mu F$.

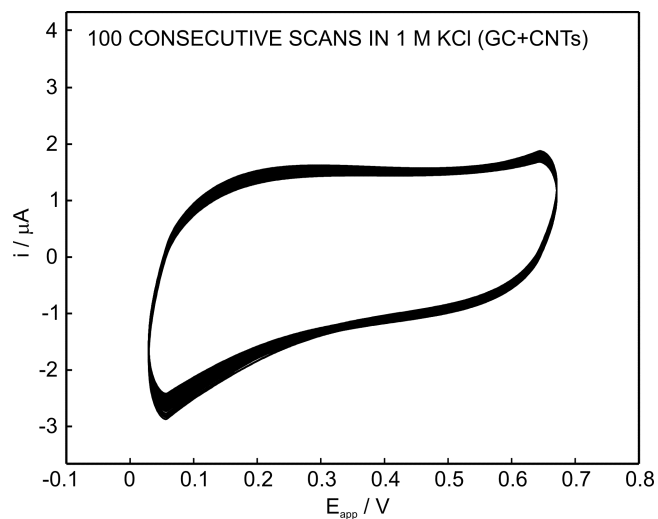


Figure S8. 100 consecutive voltammograms in 1M KCl of GC/f-MWCNTs layer. The capacitive current sampled at 0.45V decreases in 2.6%.

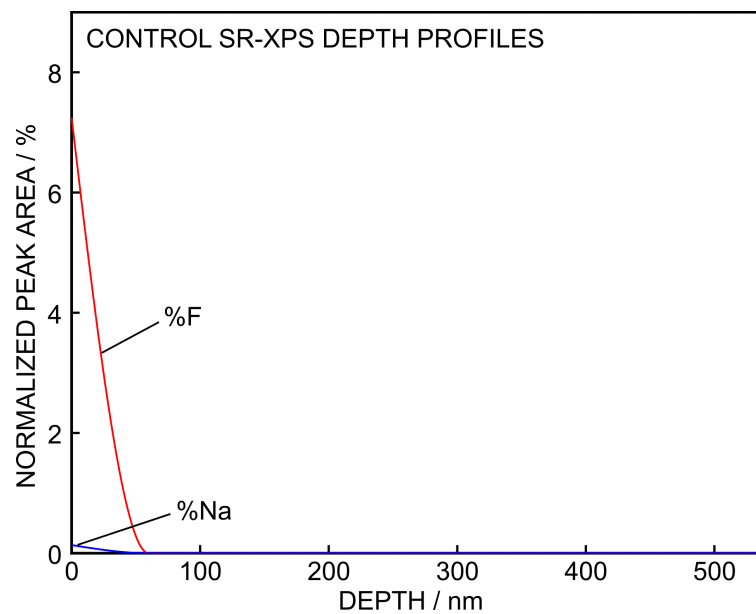


Figure S9. SXR-AS depths profiles in air using a PVC/f-MWCNT/GC electrode.

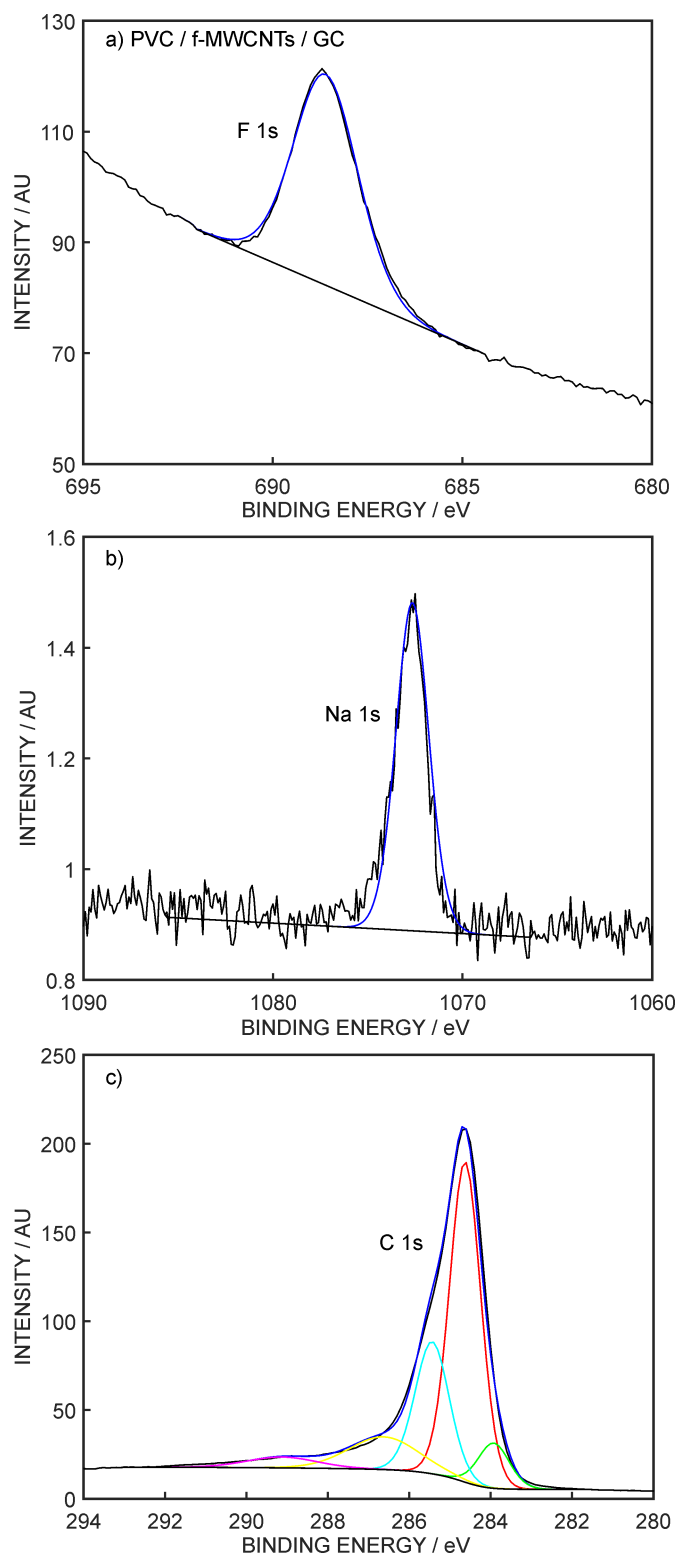


Figure S10. High resolution SR-XPS spectra (AU = counts/ 10^3) for (a) F 1s, (b) Na 1s and (c) C 1s core levels detected at the boundary between the PVC membrane and ODA MWCNT solid contact layer (i.e., at a sputtering depth of 180 nm) at an electrochemically polarized PVC/ODA MWCNT/GC electrode at 0.6 V for 180 s.

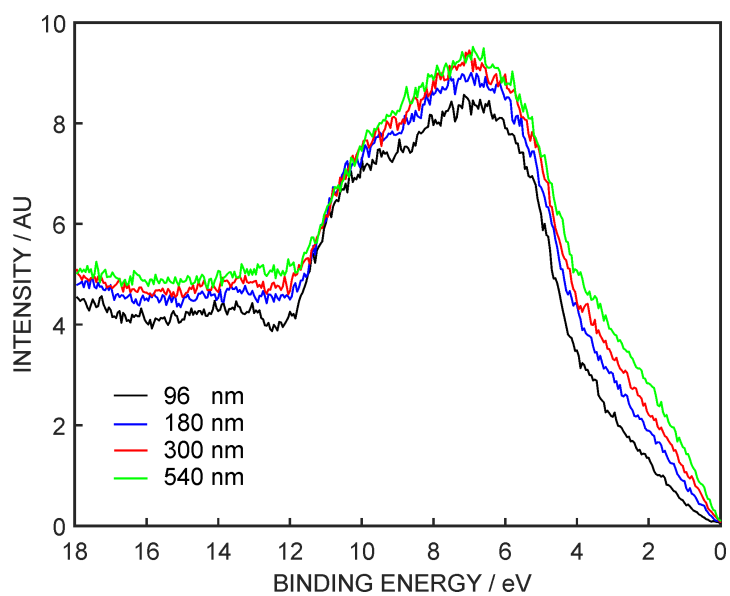


Figure S11. VB spectra (AU = counts/ 10^3) for a plasticized PVC membrane/ODA functionalized MWCNT solid contact sensor that had been electrochemically polarized at 0.6 V for 180 s as a function of Ar ion sputtering, noting that this represents the ODA functionalized MWCNT film (8-45 min or 96-540 nm).

5. References

1. Yuan, D.; Anthis, A.H.C.; Afshar, M.G.; Pankratova, N.; Cuartero, M.; Crespo, G.A.; Bakker, E. *Anal. Chem.* **2015**, *87*, 8640–8645.
2. Elliott, I.; Doyle, C.; Andrade, J.D., *J. Electron Spectrosc. Relat. Phenom.* **1983**, *28*, 303-316.
3. *In* SPECS Phoibus 150 Surface Nano Analysis Gmbh, Berlin Germany, Data Processing Section, 2011, pp. 11.
4. Seah, M.P.; Dench, W.A., *Surf. Interface Anal.* **1979**, *1*, 2-11.